CFD Modeling to Determine Forced Convection Heat Transfer on an Inclined Plate

A final project for ME548

Submitted by: Adam Scherba on March 18, 2010

Overview

The goal of this project is to determine convective heat transfer coefficients for flow over a photovoltaic (PV) solar array. This is part of a larger project where the overall energy balance of a green roof with integrated solar panels is being studied. The actual rooftop geometry has been simplified to a single inclined flat plate over a smooth ground surface. This is expected to provide a reasonable approximation of the actual flow field and heat transfer parameters. Heat transfer coefficients extracted from the CFD simulation will be compared to empirical correlations and published values found in the literature.

CFD Model

The actual geometry seen on the rooftop was simplified to create a reasonably accurate CFD model. The rooftop installation includes four green roof trays, each with four PV panels. The CFD model is representative of a single green roof tray, and a single PV surface which is dimensionally equivalent to the four PV panels of the actual installation. Figure 1 shows a comparison between the actual geometry and the model used for this simulation. Boundary conditions are discussed in detail below.

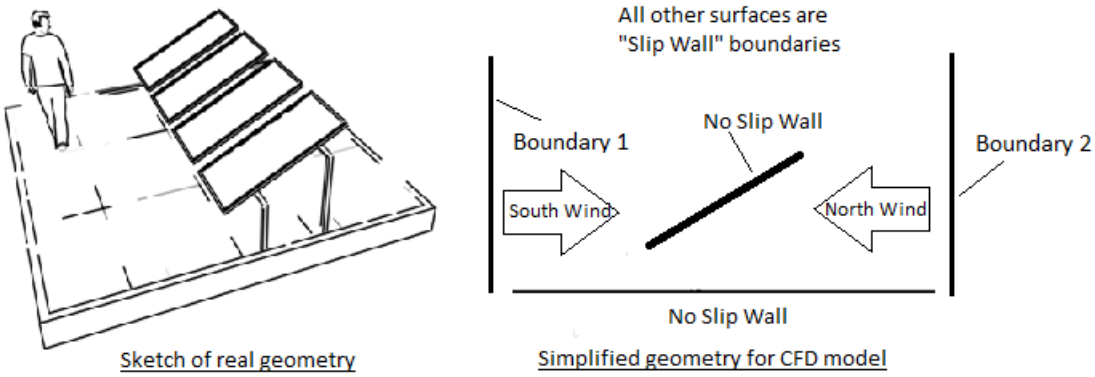

Figure 1: Geometry was simplified to a single 3D angled plate, which is representative of the four cell PV array shown on the left. Boundary conditions are shown, with boundaries 1 and 2 specified as velocity inlet and pressure outlet dependent on wind direction.

Dimensions

Dimensions used for this model are shown in Figure 2. The PV dimensions are almost identical to the physical geometry being studied on the rooftop. The fluid domain size was chosen to isolate the PV panel from any affects of the walls or other boundary conditions.

W1	Domain Width	7 m
L1	Domain Length	8 m
H1	Domain Height	3.5 m
L2	PV Length	1.6 m
(not pictured)	PV Thickness	0.034 m
W2	PV Width	3.3 m
(not pictured)	Ground plane to PV bottom edge	0.2 m

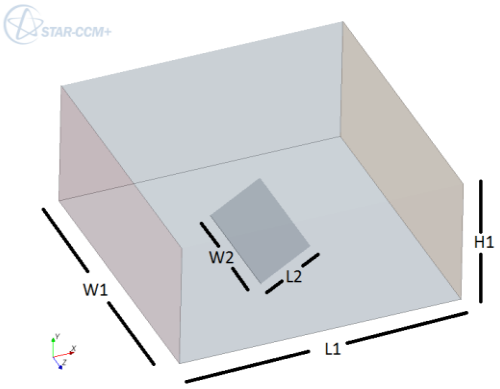

Figure 2: Primary dimensions used for the CFD model.

Boundary Conditions

The selection and assignment of boundary conditions is discussed in Table 1 below. The geometry of the fluid domain was chosen to minimize interaction between flow around the PV panel with the boundary at the walls and top of the domain. With this assumption, a slip wall was used for these boundaries due to its ease of implementation and minimal impact of the flow field.

Table 1: Comparison of physical boundaries to CFD boundary selection.

Boundary	Physical Description	CFD Boundary Applied
Inlet	Wind speed and direction on the roof are variable. Average velocities range from 0-10 m/s. This means that the "inlet" could be located anywhere with a variable velocity vector. Additionally, the incoming air is affected by the surrounding topology and is expected to be somewhat turbulent and exhibit a non-constant velocity profile. Incoming air temperatures range from approximately 0 - 35 C.	A constant velocity inlet was applied on either boundary 1 or boundary 2 (Figure 1). This allowed simulation of two wind directions. Simulations were conducted at 1, 2, and 3 m/s. The inlet temperature was set to 20 C. For future studies, the impact of a parabolic velocity profile and various turbulence intensities can be investigated.
Outlet	The "outlet" of the physical domain is nominally opposite the inlet at a given moment in time. However, the fluid will take a path of least resistance across the PV panels resulting in lateral and vertical fluid motion.	A zero pressure outlet was applied opposite the inlet (either boundary 1 or boundary 2 dependent on flow direction). The assumption is made that the fluid domain in large enough that any separation caused by the PV panel does not interact with the boundaries. All flow is expected to reach this outlet traveling in the free stream direction.

Ground Plane	The ground plane is a green roof planted with an array of plants ranging from 0.1 to 0.3 meters in height. The temperature of the plant canopy is variable, but generally slightly higher than ambient.	A no-slip wall was applied on the ground plane, with a default “smooth” roughness. This is a simplification of the actual ground plane, and future work is required to analyze the sensitivity of the model to variable ground surface roughness. The smooth wall is expected to produce a smaller boundary layer and less turbulent flow than would be seen over an actual green roof.
PV Panel	The PV panels are a smooth dark surface, exposed to solar radiation. Panel surface temperature is a function of both ambient air temperature and solar insolation. A typical summertime surface temperature is 50 C. Each green roof tray has four PV panels spaced 5 cm apart.	A no-slip wall was applied to the PV panel surfaces. The default “smooth” roughness was specified. Any airflow between panels is not accounted for since the model includes only a single representative panel. The actual thermal condition was simplified by specifying a constant temperature boundary of 50 C. This is not entirely realistic, as one would expect higher temperatures in the center of the panel, with lower temperatures along the perimeter where heat is more easily released. However, the thermal conductivity of the panel will tend to equalize the temperature distribution.
Top of Fluid Domain	The flow is completely unrestricted at the top boundary. Laminar flow in the dominant wind direction is expected at sufficient elevation where the influence of the PV panels becomes negligible.	A slip wall was applied at the top of the fluid domain. The effect of this is relatively constant velocity on the wall with no boundary layer formation. The wall condition does not allow any mass to enter or leave the boundary. If the domain is assumed to be large enough that air is only flowing in the dominant wind direction, no mass transfer is expected at the boundary.
Sides of Fluid Domain	The flow is completely unrestricted at the side boundaries. Laminar flow in the dominant wind direction is expected at sufficient distance where the influence of the PV panels becomes negligible.	A slip wall was applied at the sides of the fluid domain. The same assumptions apply as for the “Top of Fluid Domain”. The model does not attempt to capture any interaction between the array of PV panels seen on the actual rooftop (four trays in a row).

Physical Conditions

The physics parameters shown in Table 2 were chosen for their fast computation time and relatively accurate representation of the actual flow characteristics. With relatively low velocities corresponding to average wind speeds seen on the Science Building II roof, turbulence is not expected to play a big role in the heat transfer of this model. If adjustments were made to the inlet condition in an attempt to accurately model the urban boundary layer, perhaps a more robust turbulence model would be desired.

The specification of gravity and an ideal gas law was necessary to accurately capture the buoyancy driven free convection occurring between the warm PV panel and the surrounding fluid.

Table 2: Physics model selection and parameters.

Physics Model	Prescribed Parameters/Discussion
3D, Steady State, Incompressible, Ideal Gas	The actual flow characteristics are not steady state. Changes in solar radiation will result in changing ground and solar panel temperature, leading to transient values. For simplification a steady state model was selected. At typical wind speeds heat transfer is dominated by forced convection; therefore, steady state temperature should have a minimal impact on the heat transfer coefficient. Wind speed and direction are also unsteady. This analysis assumes a constant wind speed with a fixed direction.
K-epsilon turbulence model	Turbulence intensity = 0.01, Turbulence velocity scale = 1 m/s, Turbulent viscosity ratio = 10.
Gravity	9.8 m/s^2
Coupled Flow + Energy	Default

CFD software features

All of the CFD modeling for this project was completed in STAR CCM+, with the initial geometry generated in Solidworks. The Solidworks model used was a single volume which included only the fluid domain. This was essentially a cubic volume with the PV panel subtracted from its center. The geometry was exported from Solidworks as an IGES file, which was then imported as a surface mesh into STAR.

A 3D model was used for this simulation to accurately capture the expected tendency of flow to avoid the restriction caused by the PV panel. If a 2D model were used, it would be expected to accurately model the center of the PV panel, but would not be representative of the effects seen on the panel edges. The variation in heat transfer coefficient seen between the center and edges of the panel confirms that the 3D model is justified.

Existence of a symmetry plane down the center of the PV panel could have been exploited to reduce computational time. However, plans for future modeling include cases of cross flow and non-planar inlet flow. Under these conditions the full domain will be necessary.

Boundary conditions and parameters were specified per Table 1: Comparison of physical boundaries to CFD boundary selection., and physics conditions per Table 2. An initial velocity was set to aid in convergence, although this was not necessary for an accurate model.

CFD Mesh

Once the geometry was imported into STAR a suitable volume mesh had to be generated. This was done using the following meshing models: Surface Remesher, Surface Wrapper, Polyhedral Volume Mesher, Prism Layer Mesher. Use of the surface wrapper caused some initial problems because it had trouble recognizing the small gap between the PV panel and the ground plane; this resulted in a mesh that connected the panel to ground. Specification of "Contact Prevention" between the two surfaces resolved this problem. Additionally, some "Volumetric Control" was used to increase the number of cells around the PV to ground interface.

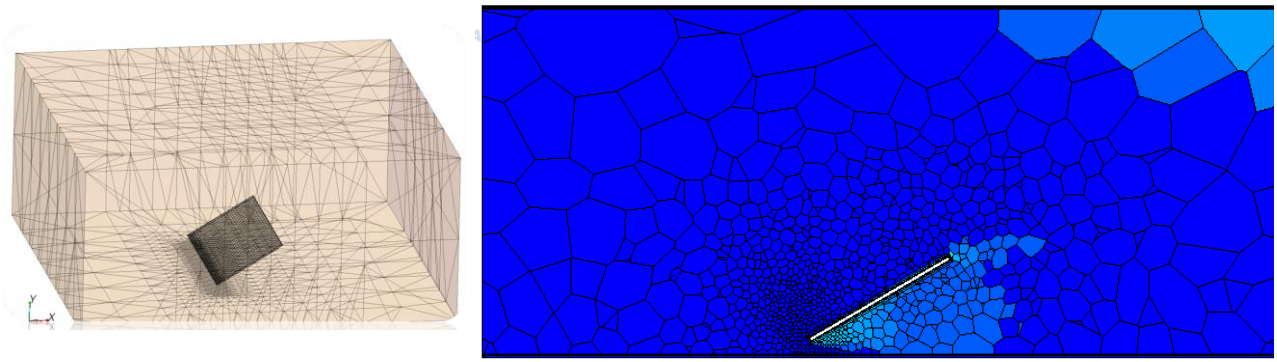

Figure 3: Mesh generated with contact prevention between panel and ground.

Results and discussion

(All figures referenced in this section are included at the end of this report)

A total of six simulations were run as shown in the Table 3 test matrix. Each simulation converged in approximately 45 minutes, or 500 iterations. In addition to monitoring the standard convergence parameters, a plot of the total heat transfer from the PV panel to the fluid was monitored. This proved to be the most valuable indicator of convergence since the heat transfer rate took slightly longer to stabilize than the other convergence parameters. An example of the typical convergence behavior is shown in Figure 4 and Figure 5.

Table 3: Experimental test matrix.

Test Matrix	
North Wind	South Wind
1 m/s	1 m/s
2 m/s	2 m/s
3 m/s	3 m/s

Although extraction of the net heat transfer coefficient was the primary goal of each simulation, plots were also generated for the mid-plane velocity, pressure, and temperature fields. Figure 6 through

Figure 8 show some results with a 3 m/s South wind, whiles Figure 9 through Figure 11 are North wind results, also at 3 m/s. A plot of the velocity field parallel to ground is shown in Figure 12.

Pressure Field (Figure 6, Figure 9)

Observation of the pressure field shows high pressure on the windward side of the PV panels, with low to negative pressure on the leeward side. Above zero pressure across most of the inlet indicates that the majority of the vertical flow regime is affected by the PV panel. Additionally, the non-constant pressure field across the top and outlet boundaries indicates that a larger control volume may be beneficial for future modeling. The fields shown here are the worst case, with less boundary interaction exhibited at lower inlet velocities. It should be noted that even for this worst case scenario, the field immediately surrounding the PV panel appears to be relatively unaffected by the control volume boundaries.

Velocity Field (Figure 7, Figure 10, Figure 12)

Observation of the velocity field is helpful to visualize the airflow immediately surrounding the PV panel. With wind from the south, a recirculation zone is found on the leeward side of the panel. Most of the air passes over the top surface of the panel, while the flow beneath the panel is accelerated due to the constriction. Flow over the top of the panel is also accelerated slightly. With a larger fluid domain slightly less flow under the panel is expected due to a path of less resistance being available above and to the sides of the panel. Additionally, if the incoming flow were subjected to a rougher ground surface or given more time to develop, a boundary layer along the ground plane would be present. The effect of this boundary layer is expected to further reduce flow below the panel.

With wind coming from the North, a large recirculation zone is seen on the leeward side of the panel. It should be noted that velocities on both sides of the panel are relatively low, while with a Southerly wind higher velocities were seen on top of the panel. This difference is discussed further as it pertains to the local heat transfer.

Figure 12 shows the velocity field on a plane located mid-way between the PV panel bottom edge and ground. This illustrates the accelerating flow seen below the panel, but also the tendency of the fluid to seek areas of less resistance by spreading towards the boundaries.

Temperature Field (Figure 8, Figure 11)

The temperature field for each flow direction is relatively similar. In both cases a wake of hot air is seen downstream of the PV panel. This wake affects the area under the panel as well as an area downstream approximately equal to the PV height (dimension L2 from Figure 2). At lower velocities this wake is still present, but the area of influence downstream is reduced.

Heat Transfer Coefficients

Instead of looking at the local heat transfer coefficient across the surface of the PV panel, the total rate of heat transfer was used to calculate a net convective heat transfer coefficient. This provides a more meaningful measure of how much heat is being transferred from the panel to its surroundings. The convective heat transfer coefficient was found by: $Q_{net} = hA(\Delta T)$, where ΔT was taken to be $T_{panel} - T_{ambient}$, and Q_{net} was extracted from STAR. Values calculated in STAR can be compared to a number of empirical correlations (Table 4).

An interesting observation is the insensitivity of the heat transfer to direction of flow. Despite very different velocity profiles, the heat transfer rate remains essentially constant. This may be due to competing modes of heat transfer. With wind from the south, the top surface of the PV panel is exposed to high velocity air that can transport a lot of heat. With wind from the north, the top surface sees air at lower velocities, but with higher levels of turbulence. The net effect seems to be that both situations result in equivalent heat transfer. This result is reinforced by experimental observations on an angled square plate, where it was discovered that plate orientation had very little impact on net heat transfer (Sparrow 1977).

Heat transfer coefficients calculated with STAR are compared to the published correlation for an angled square plate (Sparrow 1977). Sparrow showed that all of the experimental results are correlated within +/- 2.5% accuracy to the following equation: $j = 0.931 * Re^{-\frac{1}{2}}$. Here j is used for its ability to represent either heat or mass transfer. This value can easily be converted to the convective heat transfer coefficient. Other references have looked at 1 m/s air speed and measured coefficients ranging from 1.2 to 9.6 W/m^2-k (ASHRAE 1989, Anis 1983, Schott 1985, Pratt 1981).

A comparison between the coefficients calculated with STAR and the empirical correlation developed by Sparrow is presented in Table 4. Considering the range of published values at 1 m/s, the agreement between these values is quite acceptable.

Table 4: Summary of CFD calculated convection coefficient vs. empirically calculated values.

Direction	Velocity (m/s)	**CFD - hc (W/m^2-K)**	Empirical - hc (W/m^2-K)
South	1	**7.05**	3.63
South	2	**8.78**	5.13
South	3	**11.97**	6.28
North	1	**6.17**	3.63
North	2	**8.62**	5.13
North	3	**12.01**	6.28

Conclusion

This study produced a series of heat transfer coefficients that may be used for future study of the energy balance on a PV panel. Agreement is seen between the CFD results and previously published convection coefficients, which implies reasonable accuracy of the CFD model for predicting the thermal behavior of this geometry. Additionally, the discovery that flow direction has minimal impact on net heat transfer is substantiated by previous research (Sparrow 1977).

Despite the seemingly realistic prediction of convection coefficients, the limits of this simulation must be considered. In a flow with more turbulence or variable wind vectors the findings may differ significantly. Further simulations should be conducted aimed at investigating the sensitivity of this model to various parameters. Some of the parameters that should be considered for future study are: ground surface roughness, inlet velocity profile, turbulence intensity, inlet velocity direction, transient solar input, and non-uniform surface temperatures on the PV panel. A larger fluid domain should be considered for all future simulations.

Figures from STAR CCM+ Simulation

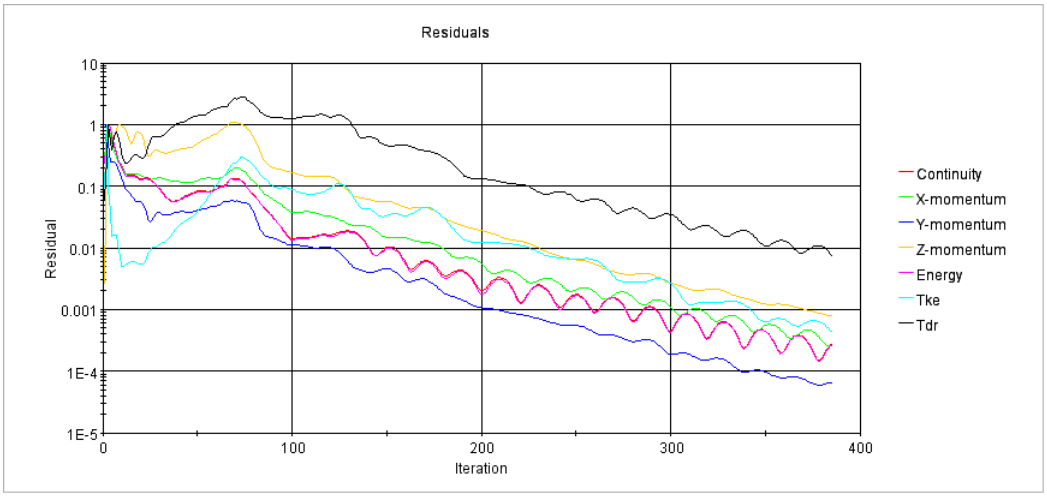

Figure 4: Typical convergence history for a simulation. Approximately 500 iterations were required.

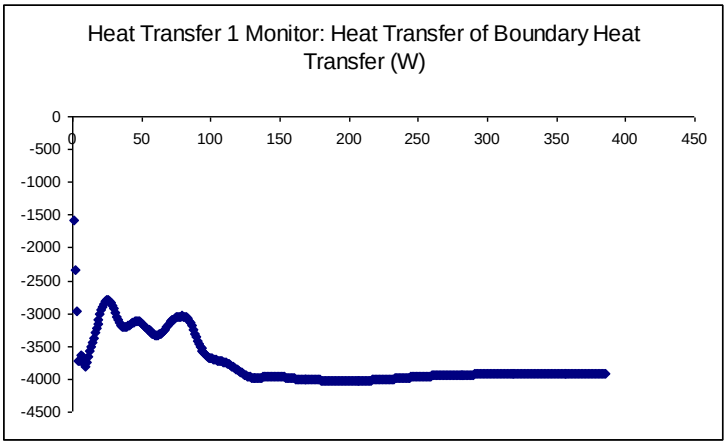

Figure 5: Convergence history for the total rate of heat transfer between the PV panel and fluid.

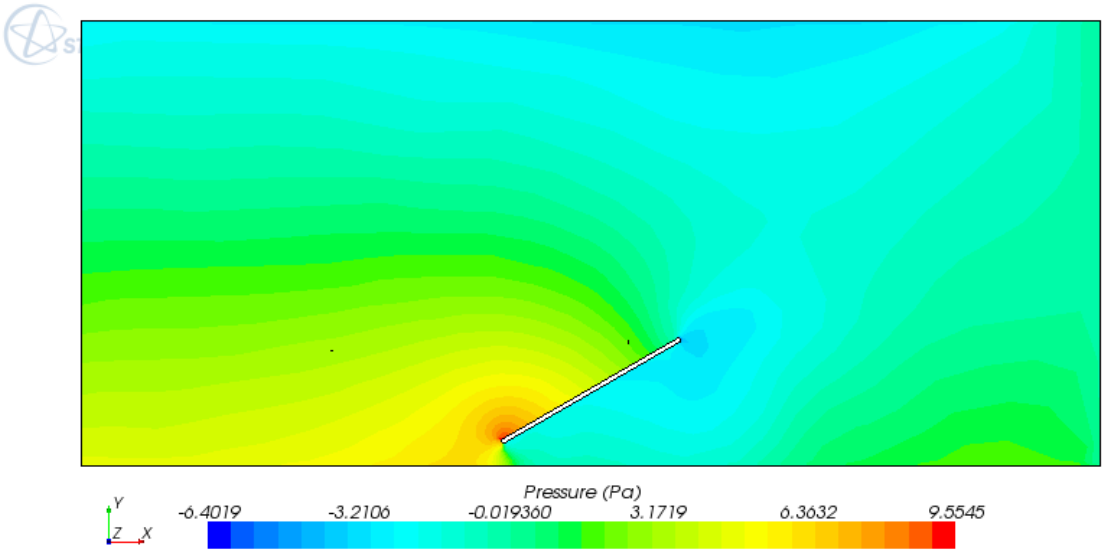

Figure 6: Mid-plane pressure distribution for 3 m/s South wind (from left to right).

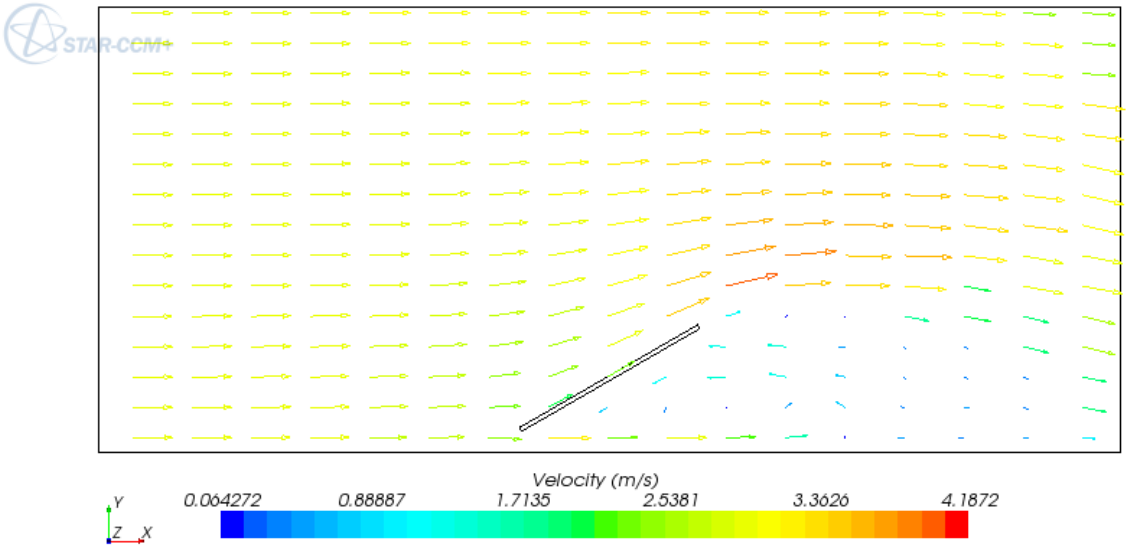

Figure 7: Mid-plane velocity field for 3 m/s South wind (from left to right).

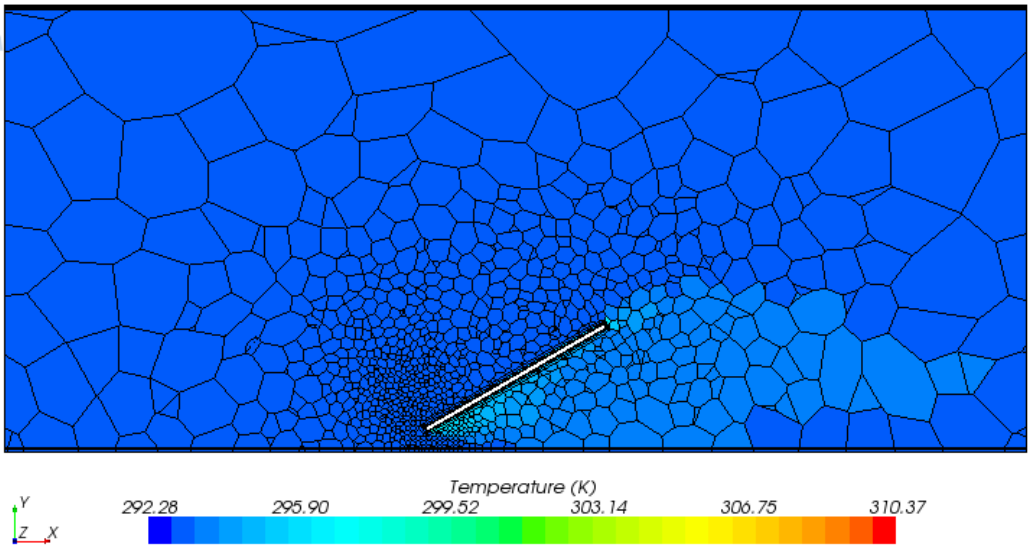

Figure 8: Mid-plane temperature distribution for 3 m/s South wind (from left to right).

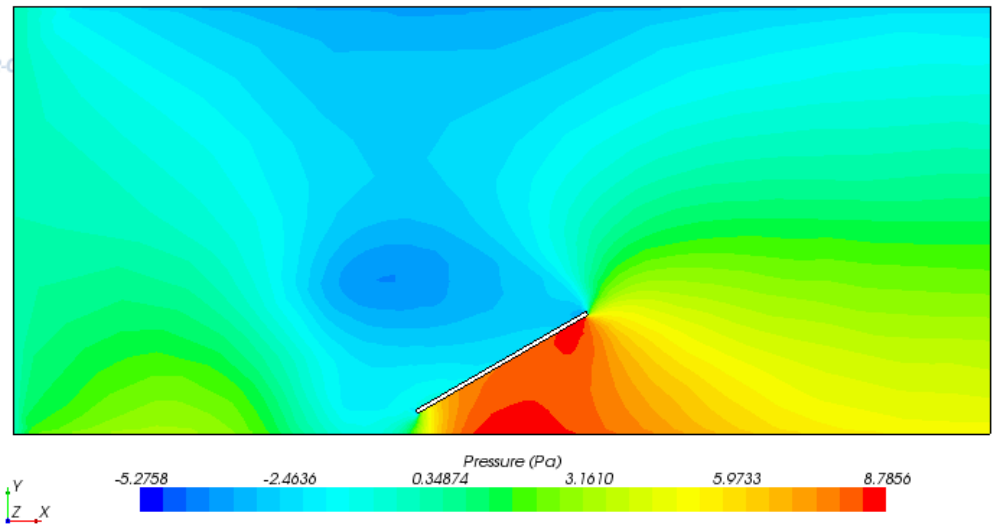

Figure 9: Mid-plane pressure distribution for 3 m/s North wind (from right to left).

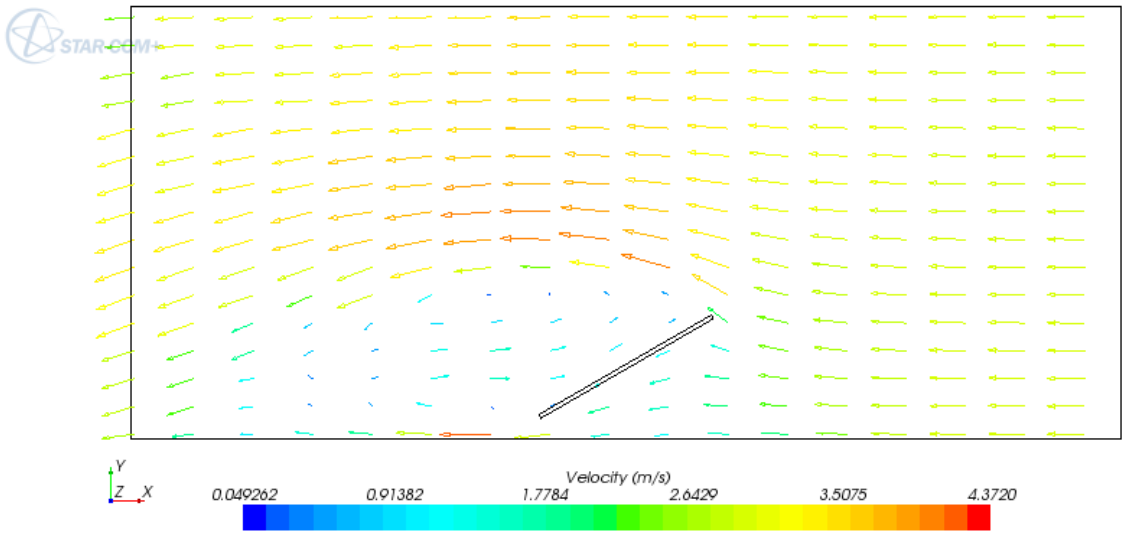

Figure 10: Mid-plane velocity field for 3 m/s North wind (from right to left).

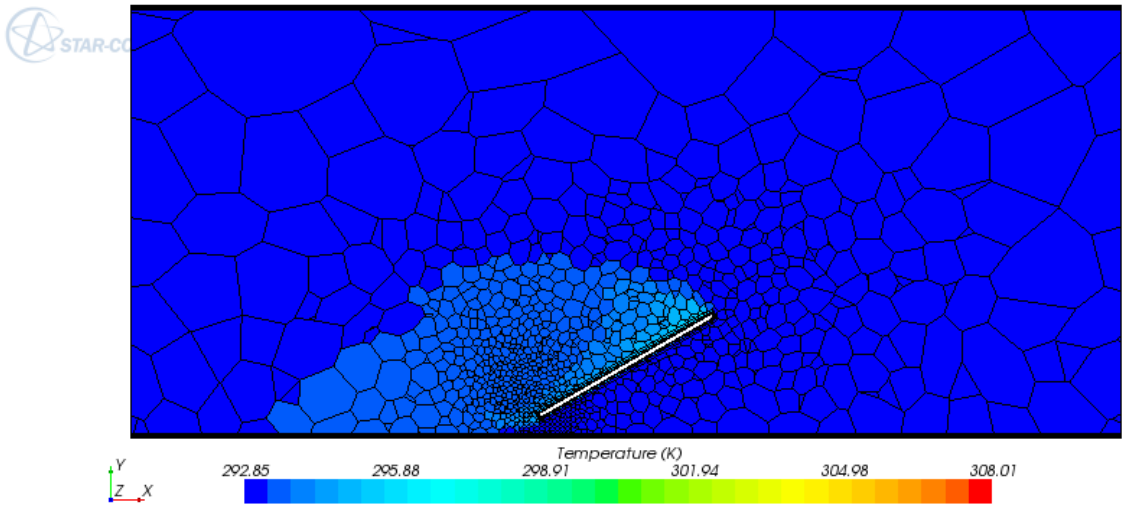

Figure 11: Mid-plane temperature distribution for 3 m/s North wind (from right to left).

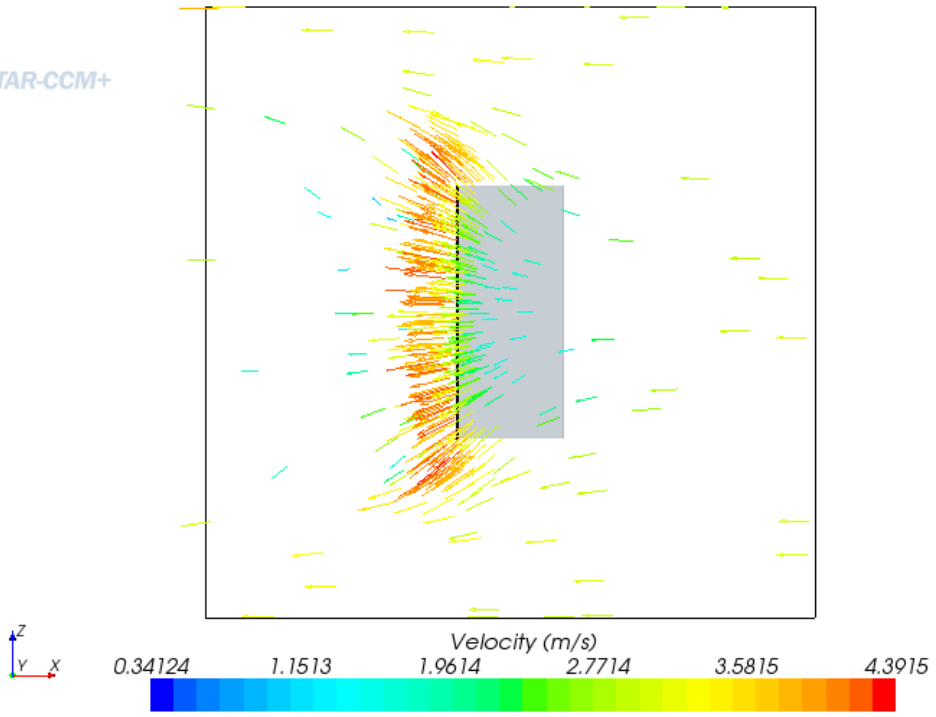

Figure 12: Velocity field mid way between ground plane and PV bottom. Wind from North at 3 m/s.

References

Anis W.R., Mertens R.P. and Van Overstaeten R. 1977. "Calculation of solar cell operating temperature in a flat plate PV array". Proc. PV Solar Energy Conference, pp 520-524.

ASHRAE. 1989. "ASHRAE Handbook: Fundamentals".

Pratt A.W. 1981. "Heat Transmission in Buildings". Wiley, London.

Schott T. 1985. "Operational Temperature of PV modules". Proc. PV Solar Energy Conference, pp. 392-396.

Sparrow, E.M. and Tien, K.K. 1977. "Forced Convection Heat Transfer at an Inclined and Yawed Square Plate – Applications to Solar Collectors." J. Heat Transfer, Vol 99, No. 4, pp 507-512.